Integrating suspended quantum dot circuits for applications in nanomechanics

J. Kirschbaum, E. M. Höhberger,[a] and R. H. Blick
Center for Nanoscience and Sektion Physik, Ludwig-Maximilians-Universität München, D-80539 München, Germany

W. Wegscheider[b] and M. Bichler
Walter-Schottky-Institut, Technische Universität München, D-85747 Garching, Germany

We present an integrated nanoelectromechanical circuit designed for achieving ultrasensitive displacement detection. It consists of a suspended quantum dot defined in the two-dimensional electron system of an AlGaAs/GaAs heterostructure and a mechanical resonator located in close vicinity. Operation of the individual components is demonstrated: Mechanical as well as transport properties of the resonator and the electron system are specified, respectively. Coulomb blockade in a freely suspended quantum dot is revealed. The data are used to estimate the maximum displacement sensitivity of the device to be 0.029 $\text{Å}/\sqrt{\text{Hz}}$.
[DOI: 10.1063/1.1492302]

The past years have seen an increasing interest in nanoelectromechanical systems (NEMS). Due to the demand for highly sensitive and fast integrated sensor components technological aspects of NEMS gain more and more in importance. For instance, reaching ultimate precision in displacement detection is essential for many applications. Examples range from quantum limited displacement sensing[1] over to single electron spin resolution[2] and force detection on DNA strands,[3] as well as sensing components for communication technology.[4,5]

Another approach for ultrasensitive displacement detection is based on Coulomb blockade,[6] which allows us to discern smallest variations in the electrodynamic environment of a quantum dot. We have combined both approaches and integrated a nanomechanical resonator with a freely suspended quantum dot circuit which allows us to probe the displacement of the resonator with the resolution of the quantum dot as a highly sensitive electrometer. Contrary to the suggestion of a radio-frequency single electron transistor (rf-SET) based on similar components,[7] this does not require matching of the quantum dot impedances to a tank circuit.

The integrated nanoelectromechanical circuit is realized in a delta-doped AlGaAs/GaAs heterostructure with a two-dimensional electron gas (2DEG) located 40 nm below the sample surface. The 2DEG is embedded in a 130-nm-thick so-called active layer which is followed by 400 nm of $Al_{0.8}Ga_{0.2}As$ serving as sacrificial layer separating the active layer from the buffer. The active layer contains the quantum well being terminated by δ-doped AlGaAs followed by a cap of undoped GaAs on both sides. Freely suspended nanostructures are obtained by selectively removing the supporting sacrificial layer.

To this end, a series of processing steps was performed starting with the definition of Ohmic contacts provided by AuGeNi pads alloyed at 420 °C. Subsequently, both nanomechanical resonator and gate electrodes were definded using electron beam lithography and covered with 60 nm of Au. In a second electron beam lithography step the quantum dots were aligned within the existing Au structure and covered with a 60-nm-thick Ni etch mask. Highly anisotropic reactive ion etching with $SiCl_4$ was employed to transfer the sample geometry into the 2DEG and to simultaneously obtain well-defined resonator sidewalls. After dissolving the etch mask in a solution of Fe-(III)-chloride the sacrificial layer is removed by wet etching in 0.1% hydrofluoric acid.

The samples discussed in the following consist of a 130-nm-wide and -thick, 1.9-μm-long free-standing resonator, which is flanked by suspended single and double quantum dot structures. The device is depicted in Fig. 1(a) and, schematically, in the inset where dots and resonator are denoted by *D* and *R*, respectively. In the following, we will limit our considerations to the single dot. The separation between the dot and the beam is 200 nm, which is small enough to allow capacitive coupling between the two structures. The quantum dots are defined in a 600-nm-wide bar by two point contacts formed by pairs of symmetric indentations. The effective size of the confined 2DEG is reduced from the lithographically defined values due to edge depletion. In previous measurements on unconstricted quantum wires it has been shown that the edge depletion width, which is mainly determined by the etching parameters, is about 50 nm for our samples. We, therefore, deduce the electronic radius of the resulting dot to be 250 nm.

The nanomechanical resonator is driven magnetomotively via the Lorentz force generated by a resonant radio-frequency current along the beam in a strong perpendicular magnetic field. The resulting motion is monitored in the reflected power by a network analyzer combined with a scattering parameter test set. The setup is depicted schematically in Fig. 1(a) and has been described in more detail previously.[8] The displayed resonator produced resonances at seven frequencies between 42 and 99 MHz. The most pro-

[a]Electronic mail: Eva.Hoehberger@physik.uni-muenchen.de
[b]Present address: Institut für Angewandte und Experimentelle Physik, Universität Regensburg, D-93040 Regensburg, Germany.

0003-6951/2002/81(2)/280/3/$19.00

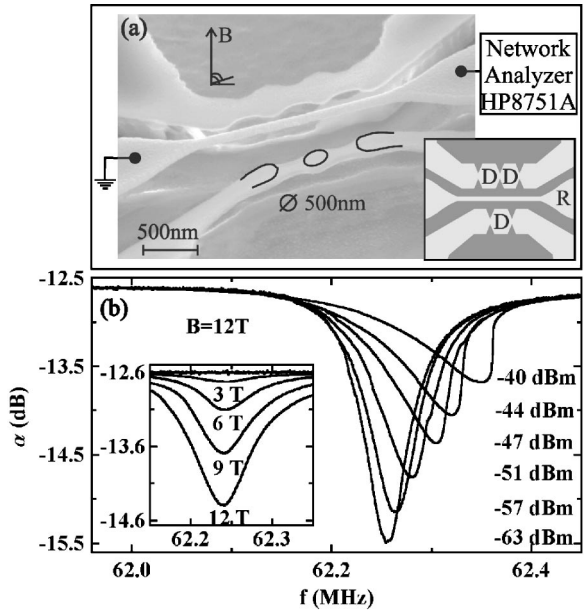

FIG. 1. (a) Scanning electron micrograph of a suspended nanostructure integrating a nanomechanical resonator and single and double quantum dots defined by symmetric indentations taken under an angle of 65°. A schematic top view is shown in the inset. (b) Mechanical resonance of the beam for an incident power between $P=-63$ and -40 dBm and a perpendicular magnetic field of $B=12$ T at $T=1.5$ K. Inset shows the magnetic field dependence.

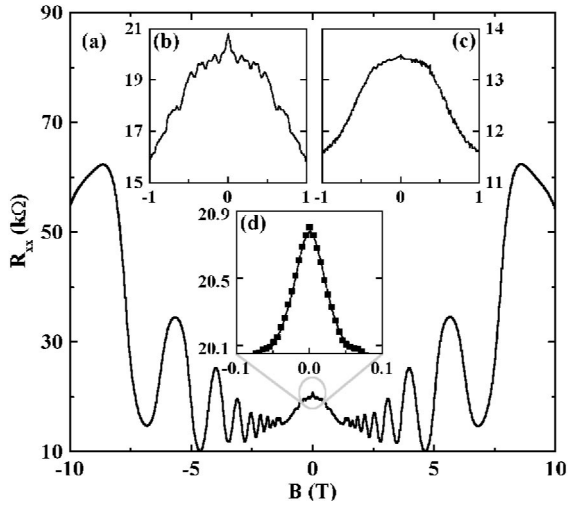

FIG. 2. (a) Shubnikov–de Haas oscillations measured at 6 K for a freely suspended cavity. Inset (b) shows an expanded view of the low-field magnetoresistance. For comparison, a magnetoresistance trace of a similar but unsuspended sample is displayed in the adjacent inset (c). (d) displays the details of the coherent backscattering peak (squares) as well as the Lorentzian fit (solid line).

nounced resonance at 62.25 MHz is shown in Fig. 1(b). A Lorentzian resonance with a quality factor of $Q=1200$ is observed at an incident power of -63 dBm in a field of $B=12$ T at 1.5 K. When increasing the incident power up to -40 dBm a strong nonlinearity develops as can be seen from the asymmetric peak shape.[8] The magnetic field dependence of the resonance at -54 dBm is illustrated in the inset.

Sheet density and mobility of the embedded 2DEG amount to $n_s=9.1\times10^{15}$ m^{-2} and $\mu=23.4$ m^2/V s. This leads to a mean-free path of 3.7 μm, which is much larger than the sample dimensions, i.e., transport through the dot is ballistic. Four-terminal measurements on suspended Hall bars have confirmed this result also for the case of readily processed samples.[9] Under normal conditions the point contacts contain a few transport channels so that the open dot can be considered as a ballistic cavity. Two gate electrodes are available to modify transport through this cavity: the resonator under dc bias as well as the backgate. Under application of a negative voltage to any of these gate electrodes the point contacts are depleted further, transforming into tunneling barriers. As a result, the dot gets separated from the reservoirs, thus entering the Coulomb blockade regime.

In order to characterize the 2DEG, two-terminal magnetotransport measurements were performed on the open quantum dot structures in a perpendicular field up to ±10 T: Fig. 2(a) displays Shubnikov–de Haas oscillations measured in a freely suspended sample at 6 K. Via the relation $n_s=g_s e/h\Delta(1/B)$, with $g_s=2$ being the spin degeneracy factor, an electron density of $n_s=5.9\times10^{15}$ m^{-2} is obtained, which is lower than the original sheet density due to deterioration of the electron gas during the etching process.

The low-field magnetoresistance for two different samples is expanded in Figs. 2(b) and 2(c). Whereas (b) magnifies the central region of the large plot, (c) shows the resulting curve for a similar but unsuspended sample. All traces are symmetric in the magnetic field $R(B)\approx R(-B)$, which implies that the magnetoresistance originates from the cavity and not from the leads. Qualitatively, the magnetoresistance traces for both samples display a similar structure. A slowly varying negative magnetoresistance, which decreases $\sim B^{-2}$, is observed at fields below 1 T. This behavior is attributed to electron–electron interaction on a lengthscale larger than the dot.[10] At higher magnetic fields ($\omega_c\tau\gg1$) Shubnikov–de Haas oscillations are resolved. The striking difference between the supported dot in Fig. 2(c) and the suspended one in Fig. 2(b) is the structure, which is superimposed on the negative magnetoresistance. Whereas the magnetoresistance decreases strictly monotonic in (c), additional features are apparent in all of the investigated suspended samples, which is explained by an enhanced boundary roughness induced by the wet-etching step.

The most prominent feature of the suspended samples is the zero-field peak magnified in Fig. 2(d). Its origin can be accounted to coherent backscattering in the cavity, analogous to weak localization in diffusive electron systems.[11] For ballistic systems it has been shown that the shape of the coherent backscattering peak is Lorentzian for chaotic and linear for regular cavities.[12] Although the investigated dots are barely elliptical all zero-field peaks can be fitted with a Lorentzian [solid line in Fig. 2(d)]. This is explained by small-angle scattering and boundary roughness scattering producing disorder even in the ballistic regime.

Applying a negative dc voltage V_g to the mechanical resonator the properties of the dot can be drastically changed. Along with a decreasing width of the constrictions quantum point contacts are formed and subsequently depleted. For gate voltages in the range of -180 mV, both point contacts are depopulated and tunneling barriers are formed. In the regime of weak coupling to the reservoirs transport through the dot is restricted by single electron charging effects before the 2DEG is completely pinched off at -1.1 V. The measurements presented in Fig. 3 show Coulomb blockade ob-

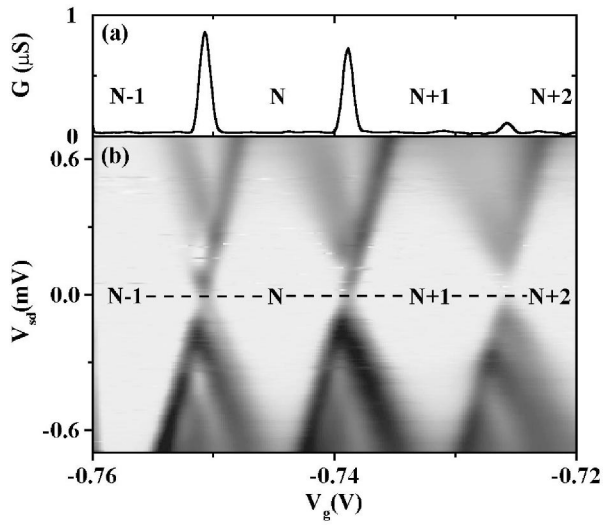

FIG. 3. (a) Coulomb blockade oscillations of the suspended quantum dot with respect to variations of the dc gate voltage V_g applied to the resonator at a perpendicular field of $B=500$ mT. (b) Gray scale plot of the differential conductance as a function of gate voltage V_g and source-drain voltage V_{sd} at $B=500$ mT showing Coulomb blockade diamonds.

served in a freely suspended quantum dot. Similar results were observed biasing the backgate instead of the resonator. Figure 3(a) displays Coulomb blockade oscillations at $V_{sd}=0$. The measurements were performed in a dilution refrigerator at $T=10$ mK using a lock-in amplifier combined with a low-noise current preamplifier. In Fig. 3(b) the differential conductance is plotted logarithmically as a function of source–drain bias V_{sd} and gate bias V_g at the resonator (white: $G=0\ \mu$S, black: $G=8\ \mu$S). Clear Coulomb blockade diamonds are resolved, which allow insight into some of the fundamental properties of the quantum dot.[6] The gate capacitance is determined to be $C_g=14$ aF by the width of the diamond. A charging energy $E_C=e^2/2C_\Sigma$ of 0.56 meV is deduced from the Coulomb gap, which corresponds to a total capacitance of $C_\Sigma=140$ aF. An estimate of the size of the dot is performed approximating the dot as a flat disk of radius R, the capacitance of which is given by $C_\Sigma=8\epsilon_r\epsilon_0 R$. With the dielectric constant $\epsilon_r=13$ for GaAs this yields a radius $R\approx 160$ nm and subsequently a number of about 480 electrons on the dot. As the negative voltage applied to the gate increases the depletion width of the 2DEG this result is consistent with the sample dimensions.

The observed Coulomb blockade oscillations can be employed to use the quantum dot as a highly sensitive electrometer. Biasing the quantum dot to the optimal operating point of maximum conductance slope we obtain a charge sensitivity of $3.3\times 10^{-4}\mathrm{e}/\sqrt{\mathrm{Hz}}$. As the induced charge on the gate is a function of the distance between the gate and the dot the system is well suited as a displacement detector. An estimate of the displacement sensitivity

$$\frac{dx}{\sqrt{\Delta f}}=\frac{\Delta I}{\sqrt{\Delta f}}\left(V_g\frac{dC_g}{dx}\right)^{-1}\frac{dQ_g}{dI}, \tag{1}$$

produces $0.029\ \text{Å}/\sqrt{\mathrm{Hz}}$ for the non-optimized device, which is an enhancement by an order of magnitude as compared to purely nanomechanical displacement detection realized previously.[8] Improving the setup might allow us to approach sensitivities of the order of $10^{-6}\ \text{Å}/\sqrt{\mathrm{Hz}}$ predicted by calculations of the shot noise limit and intrinsic displacement noise of an idealized rf-SET.[7] Vice versa, the strong coupling between resonant motion and electron transport can be employed to create a mechanical gating mechanism in addition to the familiar electrical gating to control the charging of the dot.

In conclusion, we have realized a freely suspended electron cavity in close vicinity to a nanomechanical resonator, which was depleted to form a quantum dot. Coulomb blockade has been demonstrated. Based on the deduced charge sensitivity, we expect a displacement sensitivity of $0.029\ \text{Å}/\sqrt{\mathrm{Hz}}$ with respect to the resonator displacement, which will enable mechanical gating of electron transport through the dot.

Funds from the Bundesministerium für Forschung und Technologie (BMBF) within Contract No. 01BM914 are gratefully acknowledged.

[1] P. Mohanty, D. A. Harrington, and M. L. Roukes, Physica B **284-288**, 2143 (2000).
[2] K. Wago, D. Botkin, C. S. Yannoni, and D. Rugar, Phys. Rev. B **57**, 1108 (1998).
[3] M. Rief, H. Clausen-Schaumann, and H. E. Gaub, Nat. Struct. Biol. **6**, 346 (1999).
[4] C. T.-C. Nguyen, Proceedings of the 1997 IEEE International Symposium on Circuits and Systems, Hong Kong, 9–12 June (1997), pp. 2825–2828.
[5] A. Erbe, G. Corso, H. Krömmer, A. Kraus, K. Richter, and R. H. Blick, Appl. Phys. Lett. **77**, 3102 (2000).
[6] D. V. Averin and K. K. Likharev, in *Single Charge Tunneling*, NATO ASI Ser., Ser. B **294**, 320 (1992).
[7] M. P. Blencowe and M. N. Wybourne, Appl. Phys. Lett. **77**, 3845 (2000); Y. Zhang and M. P. Blencowe, J. Appl. Phys. **91**, 4249 (2002).
[8] H. Krömmer, A. Erbe, A. Tilke, S. Manus, and R. H. Blick, Europhys. Lett. **50**, 101 (2000); F. W. Beil, L. Pescini, E. M. Höhberger, A. Kraus, A. Erbe, and R. H. Blick (unpublished).
[9] R. H. Blick, F. G. Monzon, W. Wegscheider, M. Bichler, F. Stern, and M. L. Roukes, Phys. Rev. B **62**, 17103 (2000).
[10] K. K. Choi, D. C. Tsui, and S. C. Palmateer, Phys. Rev. B **33**, 8216 (1986).
[11] J. P. Bird, D. M. Olatona, R. Newbury, R. P. Taylor, K. Ishibashi, M. Stopa, Y. Aoyagi, T. Sugano, and Y. Ochiai, Phys. Rev. B **52**, 14336 (1995).
[12] H. U. Baranger, R. A. Jalabert, and A. D. Stone, Phys. Rev. Lett. **70**, 3876 (1992).